HIGH-LATITUDE INTERMEDIATE-SCALE TEC STRUCTURE

Charles L. Rino, Brian Bretsch, Yu Morton
Smead Aerospace Engineering Sciences Department
Universtiy of Colorado
Boulder, Colorado, USA

Charles S. Carrano
Institute for Scientific Research
Boston College
Chestnut Hill, Massachusetts, USA

***Abstract*—High latitude ionospheric structure most often does not generate significant L-band amplitude scintillation. Consequently, GPS TEC measurements are nearly free of diffraction effects, which can be verified with three-frequency measurements. This paper summarizes analysis that exploit this high-latitude characteristic to investigate intermediate-scale TEC structure.**

I. Introduction

Global total electron content (TEC) maps are generated routinely by networks of GPS/GNSS receivers [1]. Global ionospheric models such as IRI [2] capture the large-scale structure characteristics. However, understanding smaller scale-dependent structure dynamics is an ongoing activity. Intermediate-scale structure from tens of kilometers to hundreds of meters is characterized by stochastic measures, most often spectral density functions (SDFs), which are formally the average intensity of Fourier decompositions of the structure. Configuration details, which impose systematic Fourier-component phase relations, are discarded, whereby the spatial distribution of the structure measures becomes more important.

Although TEC is a path-integrated measure, ionospheric penetration point maps provide spatial distribution information. Tomographic reconstruction can be used with appropriately deployed receivers. However, TEC model reconciliation most often uses whatever data are available. Regarding intermediate-scale structure interpretation, global ionospheric models are starting points for studies of quasi-deterministic structure such as traveling ionospheric disturbances and simulations of instability-driven structure. Possibly because of uncertainty in TEC resolution limits, stochastic TEC structure is just beginning to be exploited in this context.

Recent findings using three-frequency measurements show that TEC diffraction effects are negligible, even when moderate scintillation is present. Agreement between simultaneous TEC estimates made with L1-L2 and L1-L5 frequency pairs verifies that diffraction and other dispersive errors are among the smallest TEC errors. To the extent that a TEC measurement is purely path-integrated phase, the entire scale range can be interpreted as path-integrated ionospheric structure. Following our introductory remarks, we introduce wavelet-based analysis to characterize scale and position-dependent TEC structure.

II. TEC Measurement Revisited

Following the discussion in [3], the GPS phase measurements scaled to wavelength units can be written as

$$\frac{\lambda_c}{2\pi}\phi(t;f_c) = r(t) - cK\cdot TEC(t)/f_c^2 - \frac{\lambda_c}{2\pi}\phi_s\,(t;f_c) + \cdots \quad (1)$$

where $r(t)$ is the range $cK = 40.3$ TEC units, f_c is the L1, L2, or L5 center frequency and $\phi_s\,(t;f_c)$ is the phase contribution with a frequency dependence different from $1/f_c$. The ellipsis indicates additional error terms. The L1-L2 and the L1-L5 frequency pairs are comparably spaced, whereby two complementary TEC estimates can be obtained as follows:

$$\frac{\phi(t,f_{c_2})/f_{c_2} - \phi(t,f_{c_1})/f_{c_1}}{2\pi K(1/f_{c_1}^2 - 1/f_{c_2}^2)} = TEC(t) + \frac{\phi_s(t,f_{c_2})/f_{c_2} - \phi_s(t,f_{c_1})/f_{c_1}}{2\pi K(1/f_{c_1}^2 - 1/f_{c_2}^2)}, \quad (2)$$

with f_{c_1} replaced by L1 and f_{c_2} replaced by L2 or L5.

The upper frame of Figure 1 shows an example of a TEC estimates derived from a Poker Flat, Alaska GPS measurement. ΔTEC is TEC derived from (2) offset to zero at the minimum TEC level. The estimates from L12 and L15 are overlaid. The difference is shown in the lower frame. There is a trend of about 1 TEC unit, which is a known system effect. The fluctuation errors are a fraction of a TEC unit. The ramifications of multipath are under investigation.

III. Discrete Wavelet Transforms

The discrete wavelet transform (DWT) extracts octave-spaced wavelet scale estimates at $s = \Delta y 2^j$ for $j = 1, 2, ..., J$ where J is the largest power of 2 that equals or exceeds the number of samples N. A wavelet, $w(x)$ is a non-zero function over the interval $|x| < 1/2$, with zero mean, and unit intensity. Each wavelet is applied to the even number of samples that span the wavelet. The wavelet scale is identified by j with $j = 1$ corresponding to largest scale. The number of wavelet contributions varies with the scale index, j. For $j = 2$, $n = 1$ and 2 corresponding to the centers of two half segments. The smallest wavelet scale contributes $N/2$ centered samples. A discrete wavelet contribution requires a minimum of two data

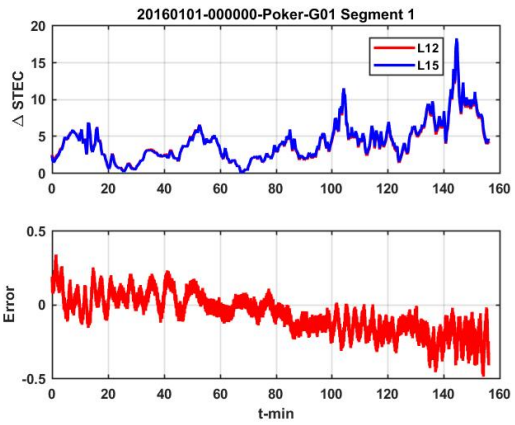

Fig. 1. Example of L12 and L15 TEC measurements from high-latitude GPS satellite measurements.

samples. The spatial frequency associated with the structure scale, s, is $q = 2\pi/s$. The DWT,

$$d_n^j = \frac{1}{2}\sum_{k=0}^{N-1} F_k \frac{1}{\sqrt{2^{j-1}}} w\left(\left(k-n\right)/2^{j-1}\right), \qquad (3)$$

can be evaluated with the same efficiency as a discrete Fourier transform. Figure 2 is a display of $|DWT = d_n^j|^2$. The number of DWT samples for each frequency scale j varies. For display purposes the value at each scale is repeated to fill in the maximum number of samples. The structure variation at a scale somewhere between 100 and 1000 sec can be identified as a transition between quasi-deterministic and stochastic variation. With wavelet decompositions, detrending or denoising is simply a selection of the wavelet scale range used to reconstruct a data example. The large scale structure is used as a mean background estimate. The fine scale is used for characterizing stochastic TEC events.

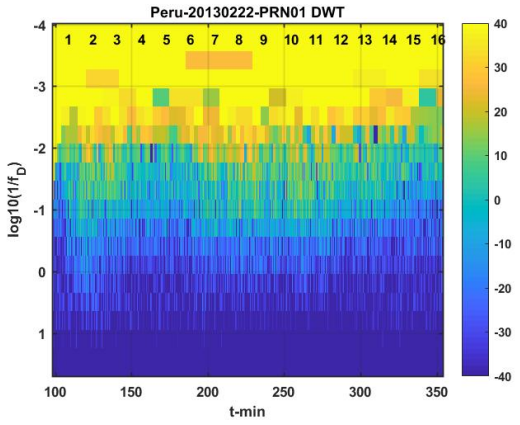

Fig. 2. Example of discrete wavelet transform.

IV. Auroral zone TEC analysis

A preliminary data set consisting of one full day of three-frequency GPS satellite passes visible at a Poker flat station were processed to extract the signal intensity, phase, and delay. A pseudo range and phase alignment procedure was used to remove the 2π ambiguity. L12 and L15 offset slant TEC measurements were extracted per (2) All of the results were similar to the example shown in Figure 1. Figure 3 shows a structure summary display of the PRN 8 satellite observed over the one day period. The left frame show the 350 km penetration point in geographic coordinates. The pentagram marks the Poker Flat station. The upper right frame shows the detrended L1 intensity. The middle and lower frames show the detrended TEC residual (center frame) and mean (lower frame).

The same wavelet-based detrending was applied to intensity and phase. However, the detrended phase is normalized by the trend to generate a constant average unity amplitude. The TEC trend and residual components are reported directly.

The data of primary interest are the TEC residuals which can be analyzed scale by scale or as scale spectra akin to smoothed periodogram estimates. The intensity variations that can be attributed to scintillation as opposed to multipath are generally too small to measure reliably at all three frequencies. In the talk the complete data set will be reviewed and evaluated for TEC structure diagnostics.

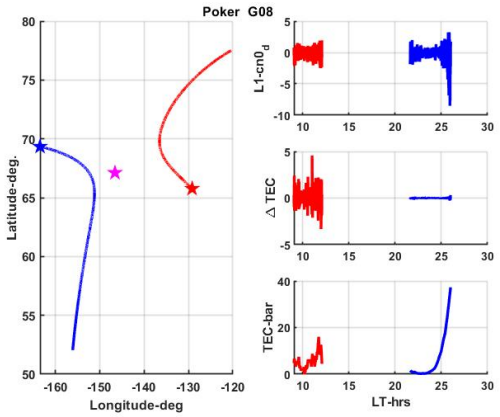

Fig. 3. Auroral zone TEC structure example

References

[1] A. Komjathy, R. Langley, and B. D., "Ingesting gps-derived tec data into the international reference ionosphere for single frequency radar altimeter ionospheric delay corrections," *Advances in Space Research*, vol. 22, pp. 793–801, 1998.

[2] D. Bilitza and B. Reinisch, "International reference ionosphere 2007: Improvements and new parameters," *Advances in Space Research*, vol. 42, p. 599609, 2015.

[3] C. Rino, B. Breitsch, Y. Morton, Y. Jaio, D. Xu, and C. Carrano, "A compact multi-frequency gnss scintillation model," *J. Ints. of Navigation*, 2018, accepted for publication.